Thermal bridges — heat flow models with Heat2, Heat3, and a general purpose 3-D solver

James B. Posey
41 Wolf Drive
Redwood Meadows, AB

W. A. Dalgliesh, P.Eng.
237 Valley Ridge Green NW
Calgary, AB

ABSTRACT

1- and 2-Dimensional analyses of steady heat flow are often used in building design to assess risk of condensation. However, many thermal bridges can only be evaluated in 3-D.

Tools available for workstations and parallel computing entail mathematical and computing expertise, if not cost, that bars their use for most building designers. Inexpensive or free heat-flow software for PCs is usually limited to 2-D.

A third possibility is desktop software for solving partial differential equations (PDEs). If one can specify the equation, or equations to be solved, the geometry and properties of the domain, and the boundary conditions, many 3-D problems can be solved on a desktop PC.

We selected one program for solving PDEs that provides for problems to be described in a high-level language. The program interprets the problem specification, creates a finite element array, solves the problem, and displays results. We used the program to describe several thermal bridges. Some were selected to allow comparison with hand calculations, or with dedicated 2-D and 3-D PC software. In these cases we found good agreement in most respects. We also used the program for problems that we could not otherwise model, and conclude that it provides a PC environment that extends the range of problems that we can consider.

INTRODUCTION

Masonry ties, metal fasteners, furring systems, intersections in light-gauge framing, structural projections, and corner conditions cannot be represented in 2-D. 3-D heat flow software for PCs is usually limited to problems that can be described as arrays of rectangular solids. We used a program, FlexPDE, that allows more general domain descriptions, capable of describing curved and inclined surfaces, to predict temperature distributions and steady-state heat flows in several thermal bridges. For some visualizations, we exported output data to VisIt, a separate data visualization program. Where possible, we compared results with predictions from dedicated heat-flow software, Heat2 and Heat3, and manual calculations. We have not used other programs with similar capabilities, e.g. Therm5 a finite element adaptive mesh dedicated heat-flow program similar in capability to Heat2, or FEMLAB, a general PDE solver.

We calculated relative temperatures of interest in cold-climate design, and comparative heat flows for the following details:

- Side-mounted brick tie on a steel stud with exterior XPS sheathing.
- Corner balcony cantilevered from concrete frame, with interior-insulated concrete walls.
- Corner balcony cantilevered from concrete frame, with exterior-insulated concrete walls.
- Corner condition, without balcony, with wall insulation on the interior.
- Corner condition, without balcony, with wall insulation on the exterior including slab edge.
- Lag bolts securing furring and exterior insulation to an uninsulated wood-frame.

METHODOLOGY

Nomenclature

T	temperature, K or C
λ, or k	thermal conductivity, $W \cdot m^{-1} \cdot K^{-1}$, or kSI
ΔT	total air temperature difference between exterior and interior
TI	Temperature Index: temperature at a point, expressed as fraction of ΔT above exterior T
F_s	shell factor, used in some models to increase thickness of thin shells, and to decrease λ proportionately when flow orthogonal to shell is expected to be negligible.

Mathematics

For steady state heat flow without internal heat sources or sinks the governing equation is $\nabla \cdot (-\lambda(x, y, z)\nabla T) = 0$. In dedicated heat-flow software there is no need to know this. In FlexPDE it can be expressed "div(-k*grad(temperature)) = 0" after declaring "k" and "temperature" as variables. Heat flow per unit area of boundary surface is found by integrating the normal component of $-\lambda\nabla T$.

Limitations

The limitations of 1-D and 2-D models are obvious where thermal bridges are concerned. To define the limits of 3-D modeling requires some exploration. If a finite difference array is used (as in Heat2 or Heat3) all surfaces have to be either parallel or orthogonal to coordinates. This makes description of curved and sloping surfaces difficult. Preliminary exploration of stepped boundaries (comparing domains orthogonal to the grid, and rotated 45 degrees) indicated that discrepancies in temperature up to 8% of ΔT, and in heat flow, up to 25%, are possible. Geometry and conductivity influence this result, but using a larger number of smaller steps does not help. Unlike an air layer, the boundary is 2-dimensional — the developed length of a stepped diagonal boundary does not change with number of steps.

With a finite element array of tetrahedra, automatically generated, another limitation appears. Models that include thick and thin elements, or small details, may become too large because of difficulties connecting the dense grid dictated by the small parts to larger elements used to fill larger spaces with shallow gradients. They may also exceed the capacity of the program to create a grid. With an adaptive grid, which is refined during solution in areas of steep gradients until an error limit is satisfied, the same problems may arise during solution. In theory, it may be possible, but in practice computer resources are often inadequate. We made an adjustment to overcome this difficulty when representing thin sections with high thermal conductivity embedded in thick sections with low thermal conductivity (e.g. metal studs in batt insulation). Because we expected the principal direction of heat flow in the thin sections to be parallel to their surfaces, we multiplied the thickness by as small an F_s factor as would allow the software to construct a grid, and divided the thermal conductivity of the material by the same factor. This increased the cross section and decreased the conductivity proportionally without affecting path length, so that flow would remain the same. Where flow is at right angles, the same adjustment increases the path length, leaving the area the same, and so introduces a locally significant error. Despite this, tests with models where a solution could be found with $F_s = 1$ indicate that the overall errors thus introduced were small. In a 2-D steel stud model the reported flux dropped to 96.6% of the initial value, as shellfactor increased from 1 to 6, while the temperature reported at mid-stud on the exterior flange increased by 2.37% of ΔT. This works where we used it both because most of the heat flow is parallel to shell surfaces, and because ΔT across the thickness is small due to the high conductivity of the material. We used a kSI of 60 for Zinc-coated sheet steel after calculating heat flow through a Zinc-Steel-Zinc sandwich to find equivalent thermal resistance. The equivalent conductivities of 0.93 mm steel with Z180 Zinc coating and of 1.61 mm steel with hot-dip Zinc coating are both within 6% of this value. For structural concrete we made a similar adjustment to allow for reinforcing steel.

In FlexPDE a node can have one periodic image (a second node at an opposite boundary that is constrained to have the same values). This capability can describe a domain that can be repeated ad infinitum in one direction without mirroring, It is possible to approximate more than two boundaries that match as to flow and gradient by inserting short sections of non-periodic boundary adjacent to corners. We did not try to devise tiled models with infinite extent, however. Instead, we approximated models infinite in 2 dimensions by judicious (but arbitrary) assignment of adiabatic boundaries (boundaries with zero gradient and no flow), and by using symmetry. Heat2 and Heat3 make no provision for periodic boundaries.

The numbers of digits reported by both programs are difficult to interpret. FlexPDE often truncates trailing zeros, even when they are significant at least internally, relative to the error criteria used to terminate reiteration, or the relative to residual fluxes when integrals that should be zero are not. In other contexts, more digits are reported than can possibly be meaningful.

A more general limitation in heat-flow calculations arises from assuming a constant boundary resistance to subsume the effects of wind, convection, and radiant heat emitted and/or absorbed from surroundings. This "resistance" is not constant — it is a complex function of indoor or outdoor conditions that would, to be properly represented, surpass the complexity of the heat flow calculation within the domain of the envelope. Additional assumptions impair the accuracy of our temperature and flux predictions:

- assumed constant conductivity, neglecting variations due to moisture, temperature, and anisotropy.
- adiabatic boundary conditions assigned to arbitrary planes, where models with periodic boundaries, infinitely tiled in 2-D, might show that adiabatic surfaces between elements are curved, or not located where anticipated.
- assumed contact between materials where there might be resistance due to imperfect contact (this simplification was not dictated by software capabilities).

If all these limitations are kept in mind, they are not likely to invalidate comparisons of relative performance of different designs of thermal bridge. Although we did not explore the possibilities, Heat2, Heat3, and FlexPDE are all capable of solving time-dependent problems with temporal variation of boundary conditions. Of the three, FlexPDE is by far the most flexible: it can handle temperature-dependent thermal properties, or anisotropic material properties, for instance.

Temperature Index

We used a temperature difference of one degree in all cases, and reported temperatures as TI because this simplifies comparison of results and calculation of temperature at a point of interest for different ΔTs. (i.e. if the interior temperature is 30 °C, and the exterior temperature is -15 °C, then the temperature of a point where TI = 0.4 is $T = -15 + 0.4(30 + 15)$ or 3 °C). If double glazed windows (with Condensation Indices in the range of 0.4 - 0.6) are sweating, then one might worry about invisible parts of the wall with equal or lower TIs.

Side mounted brick ties on steel stud

We used the following components in a model of steel stud framing with side-mounted brick ties to compare results from different methods of predicting temperature and heat flux:

1. interior temperature, 1°C
2. interior boundary, RSI 0.13
3. 12.7 mm gypsum board, kSI 0.15
4. 152 mm batt insulation, kSI 0.033, with 0.93 mm metal studs at 600 mm o.c., kSI 60
5. 50 mm XPS sheathing, kSI 0.026
6. 50 x 170 x 1.61 mm ties mounted on stud web at 400 mm o.c., projecting 18 mm beyond face of XPS, kSI 60
7. exterior boundary, RSI 0.04
8. exterior temperature, 0°C

The vapour barrier, vented airspace, wire ties, and brick veneer normally included in a wall assembly are not represented. We used several methods to predict steady state flow through the projected area of the wall, and also to predict minimum temperature at the inner sheathing surface. Of the methods used, only

FlexPDE could represent a tie with circular holes in 3-D. Heat3 could represent a plain tie (or one with rectangular holes), but not circular holes. The finite element array constructed by FlexPDE is illustrated in Figure 1b (as visualized with VisIt). The mesh for interior drywall is coloured aqua, batt insulation is blue, XPS insulation is yellow-green, and steel is meshed in red. A full stud space is represented, because the stud is asymmetric. To take advantage of symmetry, only half of a tie and half of the space between ties are represented. For the stud and tie, $F_s = 4$ A rendering of what the model represents is shown in Figure 2a. The resulting temperatures are represented in Figures 2b and 3.

FIGURE 1
Finite element array for side-mounted brick tie, overall view and detail of tie

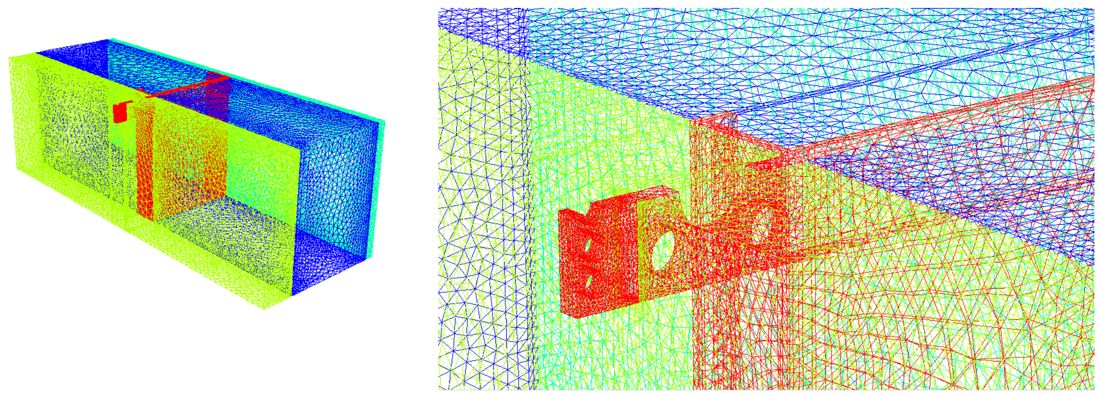

a. Perspective view of side-mount ties   b. Computational model and grid for side-mount tie on steel stud

Corners with and without balconies

These models were designed to quantify heat loss through a cantilevered balcony, and to show how the choice between indoor or exterior insulation of concrete structures affects interior surface temperatures. The first two models represent a wrap-around balcony, cantilevered from a two-way concrete slab, with concrete walls meeting at a corner. In one case there is XPS insulation on the outside of the concrete walls. In the other case, the insulation on the concrete wall is located on the interior. For comparison, the same two situations with no balcony were considered. When insulation is on the outside, it covers the edge of the floor as well as the wall. In all cases, the floor boundary is assigned a higher boundary resistance than the interior wall surface, because it will be finished with carpet or, as a ceiling, with spray texture.

The models use symmetry, so that one man's floor is another's ceiling. Only half the thickness of the slab is represented, along with half the height of the wall from floor to ceiling. They extend back from the apex of the 1.2 m wide balcony (even when omitted) a distance of 3.0 m in each direction, to an assumed adiabatic boundary. The configuration of each model is illustrated in Figures 4a, b, e, and f

1. interior temperature, 1°C
2. interior wall boundaries, RSI 0.13
3. interior floor (and ceiling) boundary, RSI 0.24
4. concrete structure, kSI 3.1
5. 50 mm XPS sheathing, kSI 0.026, outside on concrete in one case, inside in the other.
6. exterior boundaries, RSI 0.04
7. exterior temperature, 0°C

Lag-bolted exterior furring

Figure 5a shows a rendering of this assembly, consisting of pairs of bolts securing 38 x 89 mm wood furring through rigid insulation and plywood sheathing to 38 x 89 mm wood framing exposed to the interior. In Figure 5b, showing the model and computational mesh, wood is indicated by blue mesh, XPS insulation by red, plywood by yellow, and the steel by aqua. The model uses symmetry to represent two bolts, side by side, of which half of one is seen, through a 38 x 89, half of which is seen, into a 38 x 89, half of which is also seen. The complete model thus consists of 3 more elements mirrored and repeated across the vertical surfaces seen in front in the illustration of the mesh. The model is 125 x 125 mm in projected area, which implies a 250 mm spacing of both furring and framing. Exterior cladding attached to the furring is not included, and both framing and sheathing are exposed on the interior. The components consist of

1. interior temperature, 1°C
2. interior boundary, RSI 0.13
3. 38 x 89 mm wood framing, kSI 0.088
4. 15.5 mm plywood, kSI 0.093
5. 50 mm XPS sheathing, kSI 0.028
6. 38 x 89 mm wood furring, kSI 0.088
7. two 3/8” nominal lag bolts, (shoulder diameter 7.9 mm, shank diameter 6.53 mm), kSI 45.3
8. exterior boundary, RSI 0.04
9. exterior temperature, 0°C

None of our modeling environments could represent the bolt in detail. Heat3 would have to represent it as square in section, with a square head. FlexPDE could represent a cylindrical shaft, with a hexagonal head, and different diameters of shoulder and shank, but not the threads nor the taper at the end, at least not with reasonable effort. The threads, and compressed wood surrounding them might be represented as concentric cylinders of materials with intermediate resistances. However, heat transfer is probably increased by the increased surface area of the threads. We had no basis for adjusting for these effects, or for determining what size of square pin would be equivalent, so we ran the model with threadless bolts in FlexPDE, and, to compare results, without any bolts in FlexPDE and Heat3. We also considered the effect of using stainless steel instead of carbon steel.

RESULTS

Side mounted brick ties on steel stud

This detail proved to be a challenge. The language of FlexPDE scripts is flexible enough that many syntactically correct descriptions of a problem are possible. However, some fail during grid construction more easily than others. For this problem, several models were tried and discarded before one that worked well was found. It was still necessary to use a F_s of 4. In Heat3, with the holes omitted, we had to adjust the successive relaxation coefficient, and accept much longer computation time to get an internal error in flux of less than 0.01%. Initial runs never reached an error of less than 1%, and eventually started to diverge; error increasing with each iteration. In FlexPDE we obtained flows by integration over the interior surface, and did not try to compare the result with flows through exterior surfaces. Figure 2b shows a colour-keyed representation of temperature contours (isothermal surfaces) in perspective, from FlexPDE, visualized with VisIt. Note that 0 degree (red in the legend) and 1 degree (light green) isosurfaces are not represented — they are outside the domain. Figure 2a shows a rendering of two ties in a similar wall assembly.

FIGURE 2
a. Perspective rendering of two ties on studs, with insulation partly cut away
b. Partial perspective view of temperature contours in side-mounted brick tie - steel stud wall

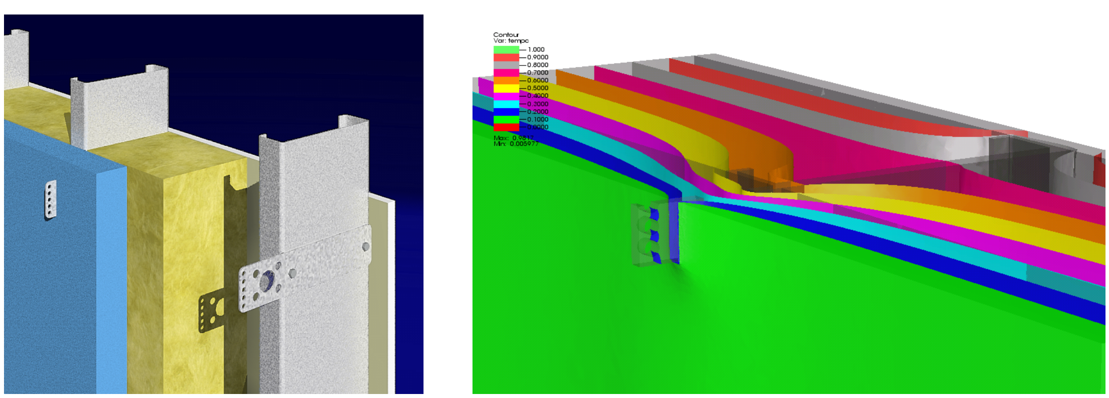

a. b.

Figure 3 shows grey-scale-keyed representations of temperature in 2D, as visualized within FlexPDE, on various planes. (Colour-keyed representations are possible, but illegible when reduced to grey-scale). The X axis is horizontal and perpendicular to the wall, Y is vertical, and Z is horizontal. The scale is different (e-2) in Figure 3a, than in Figures 3b-d.

FIGURE 3
Temperatures in steel stud wall with side-mounted brick ties

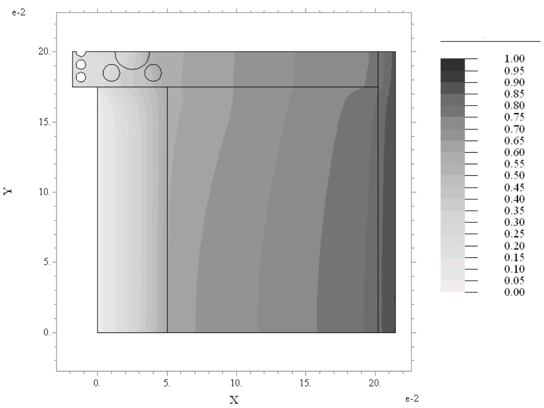

a. Temperatures at middle of tie, vertical section

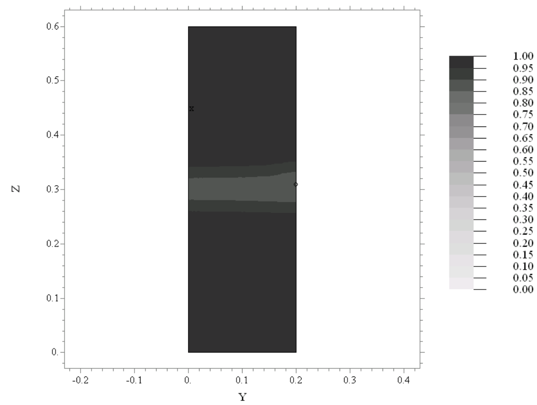

b. Temperatures on interior surface (up ⇒)

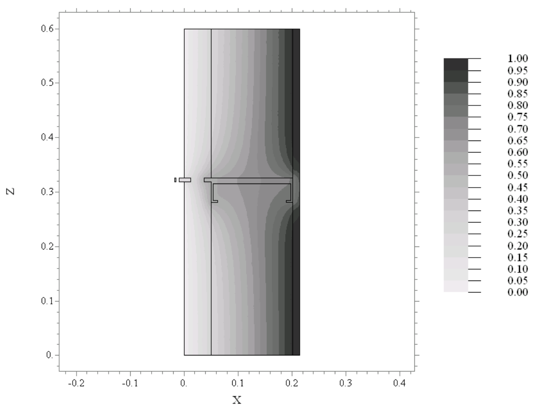

c. Temperatures at middle of tie, horizontal section

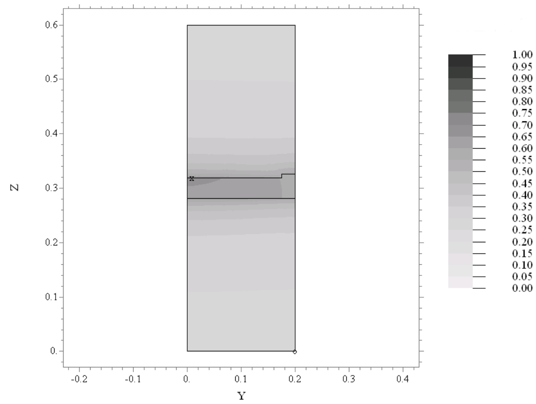

d. Temperatures on interior side of sheathing (up ⇒)

Table 1 gives numeric results for overall heat flow, and for minimum temperature on the inside surface of the XPS sheathing, as well as on the interior wall surface, for various models of the steel stud wall with side-mounted ties. In this table, the numbers of digits are as reported by the software.

TABLE 1
Results compared for side-mounted brick ties

	Model	No stud or tie	Stud, no tie	Stud + plain tie	Stud + perforated tie
Heat flow, $W \cdot m^{-2} \cdot {}^{\circ}C^{-1}$	Hand	0.14741	–	–	–
	Heat2	0.1474	0.1906	–	–
	FlexPDE, 2D, $F_s = 1$	0.147407	0.193459	–	–
	Heat3	0.1474	0.1931	0.2509	–
	FlexPDE, 3D, $F_s = 4$	0.147415	0.194218	0.257772	0.242123

TABLE 1
Results compared for side-mounted brick ties

	Model	No stud or tie	Stud, no tie	Stud + plain tie	Stud + perforated tie
Min. temperature on inside of sheathing, TI	Hand	0.28936	–	–	–
	Heat2	0.2894	0.294	–	–
	FlexPDE, 2D, $F_s = 1$	0.2894	0.295	–	–
	Heat3	0.2893	0.2956	0.2922	–
	FlexPDE, 3D, $F_s = 4$	0.2894	0.296	0.293	0.293
Min. temperature on interior wall surface, TI	Hand	0.98084	–	–	–
	Heat2	0.9808	0.9153	–	–
	FlexPDE, 2D, $F_s = 1$	0.98084	0.915	–	–
	Heat3	0.9808	0.9149	0.8509	–
	FlexPDE, 3D, $F_s = 4$	0.9807	0.915	0.844	0.855

The temperature results from these various means of calculation compare favorably. They tell us that whereas designers commonly worry about condensation on the tie or stud, it is the sheathing mid-way between studs and ties that is in greatest danger. They also indicate that heat loss when ties have perforations is about 6% less for this wall overall (or that the insertion loss for perforated ties is about 14% less than that for plain ties). Adding perforations makes little difference to critical temperatures.

Corners with and without balconies

Cantilevered balconies are structurally efficient, so the thermal consequences tend to be disregarded. When it comes to choice between inside or outside insulation, those who are used to insulating concrete structures on the interior — without problems — transport their designs to different climates without qualm. These models told us that in climates and occupancies where condensation on interior concrete surfaces is not a problem, the interior can be viewed as the best place to insulate. A given thickness of insulation, placed on the interior, will provide higher interior wall surface temperatures in cold weather, and hence greater thermal comfort. However, for colder climates or more humid interiors, placing the insulation on the exterior will raise the minimum interior concrete temperatures and reduce the risk of mold under the carpet, or in spraytex on ceilings (not to mention the risk of condensation behind the insulation).

Initially, we modelled corner balconies with a column in the corner, and an frame wall on one side, represented as a monolithic material with a lower k than that of concrete. This reached limits for both programs. In Heat3 we used the maximum number of boundary surfaces, and, to confirm results, also used nearly the maximum number of grid divisions. In FlexPDE, there was no problem getting temperature results, but getting good flux results and satisfying error limit criteria proved difficult. FlexPDE can report flow normal to boundaries, integrated over all boundaries, as an accuracy check for flow. Since inward and outward flows have opposite signs, this integral should be zero for a steady state problem. Flows can also be integrated surface by surface, allowing heat loss to be determined by summing integrals over all interior, or all exterior surfaces. These two sums should be equal. In practice, reported flow from interior boundaries is not equal to flow reported for exterior boundaries, and the difference is not equal to the integral over all boundaries. To get reasonable correspondence between inward and outward flows we simplified the models by removing the column and making the two walls the same. By adjusting grid constraints, and using a computer with 1 GB of RAM, we were able to improve results further. More resources might yield further improvement. However, results from the simpler models are just as informative, and with the resources available, FlexPDE computation takes minutes per run rather than hours. Figures 4a and 4e show that surfaces meeting at right angles, coupled with large differences in material properties cause a proliferation of small elements in the adaptive mesh.

Heat3 and FlexPDE produced similar results with the simplified models. Figure 4 shows the configuration of materials (with dark mesh for concrete and light mesh for insulation), and corresponding temperature maps, from FlexPDE via VisIt, for the four models. Table 2 shows comparative numeric results. For heat

FIGURE 4
Configurations and temperatures: concrete wall and slab corners, with and without balconies, insulated on inside, or outside

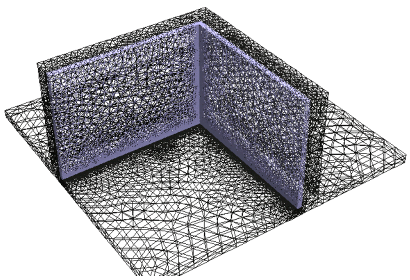

a. Configuration with balcony, insulation inside

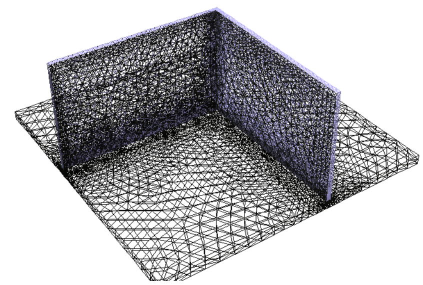

b. Configuration with balcony, insulation outside

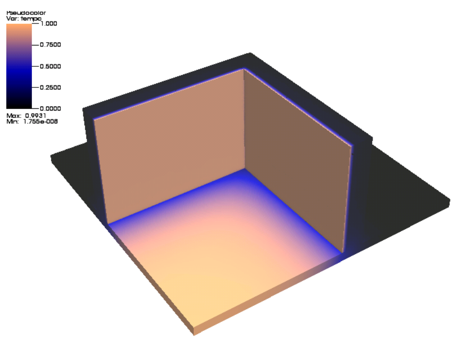

c. Surface temperature distribution, insulation inside

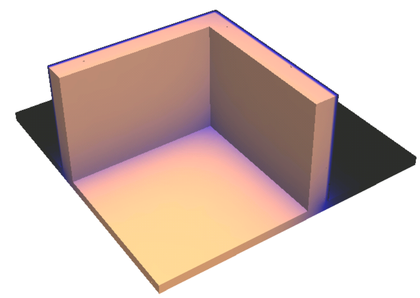

d. Surface temperature distribution, insulation outside

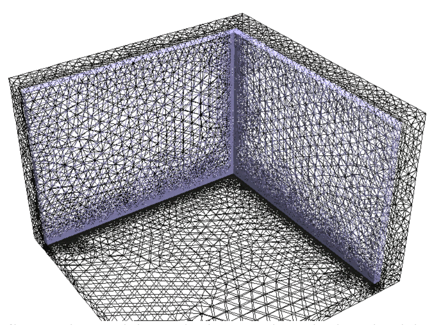

e. Configuration with no balcony, insulation inside

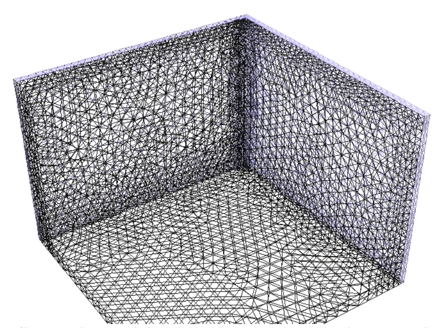

f. Configuration with no balcony, insulation outside

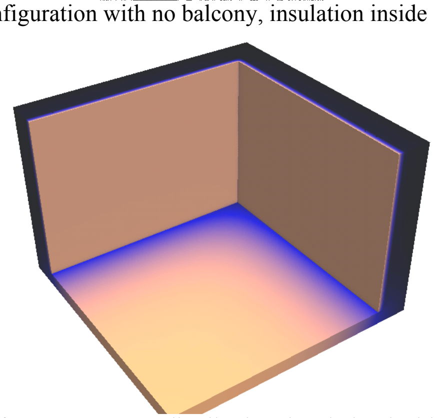

g. Surface temperature distribution, insulation inside

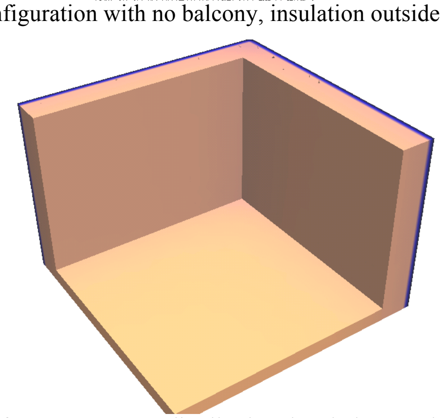

h. Surface temperature distribution, insulation outside flow, Heat 3 reports two numbers — flow through the system and residual error. In FlexPDE we had to identify each boundary surface individually and ask for the individual integrals. “FlexPDE in” is the sum of sums for those surfaces we specified as interior. “FlexPDE out” is the sum of sums for exterior surfaces. The net flow is the integral FlexPDE reports for all surfaces, including those specified as adiabatic. In a perfect model the difference between “in” and “out” would equal the net, and be 0. Although this is not the case, the results agree well for comparative purposes, although not as well for flows as for temperatures.

TABLE 2
Results compared for corners with and without balconies

Result	Model	Balcony		No Balcony	
		Insulation inside	Insulation outside	Insulation inside	Insulation outside
Heat flow, $W{\cdot}°C^{-1}$	Heat3 FlexPDE in FlexPDE out	3.696 3.753 3.692	4.626 4.666 4.704	3.695 3.763 3.716	2.152 2.14148 2.150756
Net heat flows, $W{\cdot}°C^{-1}$	Heat3 FlexPDE	7e-5 1.45e-2	8.7e-5 4.29e-2	6.9e-5 1.11e-2	4.1e-5 1.45e-2
Min. temperature on interior surface, TI	Heat3 FlexPDE	0.208 0.210	0.601 0.601	0.211 0.210	0.897 0.89758

Lag-bolted exterior furring

Figures 5b and c show the arrangement of materials in the model, the computational grid, and the resulting temperature field, represented as surfaces of equal temperature (or TI), all as visualized in VisIt. In this case it would be interesting to know what effects varying boundary temperatures, diffusion resistance of the wood, and transient storage of condensation in the wood around the bolt, might have. In many cases, it is likely that the bolt would be below the interior dewpoint temperature. If the bolt were exposed to the interior, its surface temperature would be higher, but there would be no transient mitigation of condensation by adsorption in surrounding wood.

FIGURE 5
Lag bolts through furring and insulation to interior framing — model and result.

a. Perspective view b. Materials and computational array c. Temperature contours (carbon steel)

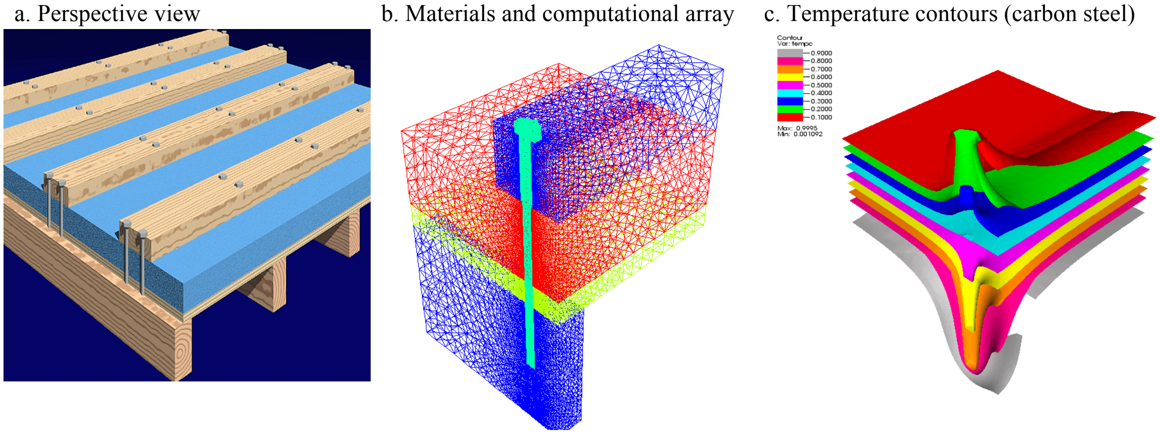

With Heat3, regardless of how long the model was allowed to run, the difference between heat entering the interior boundary, and exiting the exterior boundary remained 0.0002 W, or 0.0128 $W{\cdot}m^{-2}{\cdot}°C^{-1}$, enough to explain the discrepancy in results between the two programs. We found no adjustment of the program parameters that could improve this result. Table 3 shows results for this model with no bolt, a carbon steel bolt (kSI 45.3), and a stainless steel bolt (Type 420, kSI 26).

TABLE 3
Results compared for lag-bolted exterior furring

Result	Model	No bolts	Carbon steel bolts	Stainless steel bolts
Heat flow, $W \cdot m^{-2} \cdot {}^{\circ}C^{-1}$	Heat3 FlexPDE[a]	0.4512 0.4528	– 0.6196	– 0.5860
Min. sheathing temperature, TI	Heat3 FlexPDE	0.854 0.845	– 0.510	– 0.554
Min. interior surface temperature, TI	Heat3 FlexPDE	0.9356 0.933	– 0.839	– 0.856

a. rounded from 7 to 4 digits

Like the brick tie models, these models gave similar results where both programs could be used. When bolts are included, the minimum sheathing temperature of 0.51 suggests that for some climates and occupancies, condensation in the wood adjacent to the bolt could be a concern. Assuming an air-vapour barrier on the outside of the sheathing, the minimum sheathing temperature (where the exterior sheathing surface and bolt meet) determines what level of indoor moisture could be tolerated. Although stainless steel is about half as conductive as carbon steel, the differences in result are slight, presumably because it is still 1000 times more conductive than wood or insulation.

SUMMARY AND DISCUSSION

All the programs provide potential pitfalls. Heat3 has no objection to two objects occupying the same space. If they are of the same kind of material, the overlap will not be evident in the visualizations, and will generate no error, but the results will be wrong. In FlexPDE it is difficult to verify that the boundaries are correctly located and have the desired properties, so that it may only become evident that there is a problem when the solution is obviously wrong. There is no provision for visualization of boundary conditions — if they are not as intended, this has to be inferred from the results. With either program, results should be checked against known analytic truths, or by comparison with other methods.

Of the outputs of interest in design, temperature fields are the most rapidly and accurately obtained. Just looking at two visualizations is enough to reveal significant differences between two designs. Where there were discrepancies in temperature between programs, they were in the places where the gradients were steepest. Flows take longer to calculate, and are more prone to discrepancies between programs.

In Heat3 the user can specify the number of mesh intervals, expansion or contraction of the mesh in each region and direction, a successive over-relaxation coefficient, and a stop criterion based on temperature error, flow error, or number of iterations. FlexPDE has many more parameters that can be specified to control mesh generation, accuracy, and method of solution, but defaults save the user from having to consider most of them. In either environment, adjusting user-specified parameters that have nothing to do with the physics being modelled can change the results.

While many geometries cannot be properly represented using orthogonal grids, we found that tetrahedral grids also have limitations. Thin sections are difficult to represent, just as curved and inclined surfaces are difficult to represent in orthogonal grids. Both types of software have limitations. Each is capable of solving problems that are difficult for the other.

We conclude that the PDE-solver extends the range of 3-D thermal bridge problems that can be considered. For the purpose of comparing alternative designs, it is sufficiently accurate and compares well with dedicated finite-difference heat-flow software. It allows us to consider cases that would be impossible to model otherwise. Looking forward, it offers the possibility of adding equations and linked variables to expand the horizon of possible problems to include combined effects of moisture and heat.

REFERENCES, RESOURCES, & NOTES

ASHRAE, 1997, “1997 ASHRAE Handbook, Fundamentals, SI Edition”, American Society of Heating, Refrigerating and Air-Conditioning Engineers, Inc., Atlanta, GA.

Backstrom, Gunnar, 2004, “Fields of Physics by Finite Element Analysis — An Introduction”, GB Publishing, Malmo, Sweden.

Blomberg, Thomas, May 1996, “Heat Conduction in Two and Three Dimensions, Computer Modelling of Building Physics Applications”, Department of Building Physics, Lund University, Sweden, ISBN 91-88722-05-8. (A detailed discussion of Heat2 and Heat3.)

PDE Solutions Inc., 2004, “FlexPDE User Guide” and “FlexPDE Reference Manual, Version 4”, PDE Solutions Inc., Antioch, CA.

Lawrence Livermore National Laboratory, 2003, “VisIt Getting Started Manual, Version 1.1” and “VisIt User’s Manual, Version 1.1”, University of California, Livermore CA. (VisIt is freely available, without cost, but only for individual, non-commercial use.)